AJR FOCUS ON:

Pitfalls in Wrist and Hand Ultrasound

Mary M. Chiavaras[1]
Jon A. Jacobson[2]
Corrie M. Yablon[2]
Monica Kalume Brigido[2]
Gandikota Girish[2]

OBJECTIVE. The purpose of this article is to review a number of diagnostic pitfalls related to ultrasound evaluation of the hand and wrist. Such pitfalls relate to evaluation of tendons (extensor retinaculum, multiple tendon fascicles, tendon subluxation), inflammatory arthritis (incomplete evaluation, misinterpretation of erosions, failure to evaluate for enthesitis), carpal tunnel syndrome (inaccurate measurements, postoperative assessment), ulnar collateral ligament of the thumb (misinterpretation of the adductor aponeurosis and displaced tear), wrist ganglion cysts (incomplete evaluation and misdiagnosis), and muscle variants.

CONCLUSION. Although ultrasound has been shown to be an effective imaging method for assessment of many pathologic conditions of the wrist, knowledge of potential pitfalls is essential to avoid misdiagnosis and achieve high diagnostic accuracy.

Ultrasound can be used to evaluate tendon, muscle, ligament, bone, and joint abnormalities as a complement to other imaging methods, such as radiography, CT, and MRI [1, 2]. High accuracies can be obtained when ultrasound is performed for the proper indications by an experienced operator with thorough knowledge of anatomy and musculoskeletal ultrasound [3]. A number of potential diagnostic pitfalls should be avoided to improve accuracy and decrease interpretation errors. Such pitfalls relate to ultrasound evaluation of tendons, inflammatory arthritis, carpal tunnel syndrome, ulnar collateral ligament of the thumb, ganglion cysts, and pseudomasses.

Tendons

Pathology

One common application for musculoskeletal ultrasound in the hand and wrist is tendon assessment [4]. A normal tendon is hyperechoic with a fibrillar echotexture and uniform thickness [5]. Tendon pathology includes tenosynovitis, tendinosis, and tendon tear. Tenosynovitis is characterized by distention of the tendon sheath with anechoic or hypoechoic fluid, synovial hypertrophy (which ranges from hypoechoic to, less commonly, hyperechoic compared with subcutaneous fat), or thickening of the tendon sheath itself with possible hyperemia [4]. Anatomically, flexor tendon sheaths are present in the digits with possible proximal extension to the wrist [6]. In the palm, an ulnar bursa is present superficial to the third through fifth metacarpals, which communicates with the flexor tendon sheath of the fifth finger in 81% of cases [6]. A radial bursa is located superficial to the second metacarpal as a continuation of the flexor pollicis longus tendon sheath, and an intermediate bursa may connect the ulnar and radial bursae in 50% of cases [6]. The extensor tendon sheaths are located beneath the extensor retinaculum of the wrist, may be up to 7 cm in length, and terminate at the level of the proximal metacarpals [6].

Tendinosis is characterized by hypoechoic tendon enlargement with variable hyperemia on color or power Doppler imaging. A partial-thickness tendon tear will appear as an incomplete anechoic cleft whereas a full-thickness tendon tear will appear as complete tendon discontinuity with retraction of the torn tendon ends [4]. Dynamic evaluation improves accuracy in the diagnosis of full-thickness tendon tear; tendon movement is not translated across the site of a full-thickness tendon tear and tendon stump retraction becomes more obvious. Dynamic evaluation can also assess for tendon subluxation or dislocation.

Pitfalls

Extensor retinaculum and pseudotenosynovitis—One structure that may simulate

Keywords: anatomic variants, anatomy, wrist ultrasound

DOI:10.2214/AJR.14.12711

Received February 9, 2014; accepted after revision April 17, 2014.

[1]Department of Radiology, McMaster University, Hamilton General Hospital, Hamilton, ON, Canada.

[2]Department of Radiology, University of Michigan, 1500 E Medical Center Dr, TC2910L, Ann Arbor, MI 48109-0326. Address correspondence to J. A. Jacobson (jjacobsn@umich.edu).

AJR 2014; 203:531–540

0361–803X/14/2033–531

an abnormality is the extensor retinaculum of the wrist. This bandlike structure extends transversely over the dorsal wrist at the level of the radiocarpal joint measuring 8–23 mm in craniocaudal dimension and up to 1.7 mm in thickness [7]. The extensor retinaculum functions to stabilize the extensor tendons and keep the tendons approximated to the radius during wrist extension [8]. On ultrasound, the extensor retinaculum is slightly hypoechoic compared with the subcutaneous fat. If the ultrasound beam is angled, the retinaculum can appear more hypoechoic and may simulate tenosynovitis of the extensor tendons, especially the extensor digitorum [7] (Fig. 1A). With knowledge of the expected location of the extensor retinaculum at the radiocarpal joint and thickness, this potential pitfall can be avoided. Another pitfall that may simulate tenosynovitis is misinterpreting the normal hypoechoic muscle at the

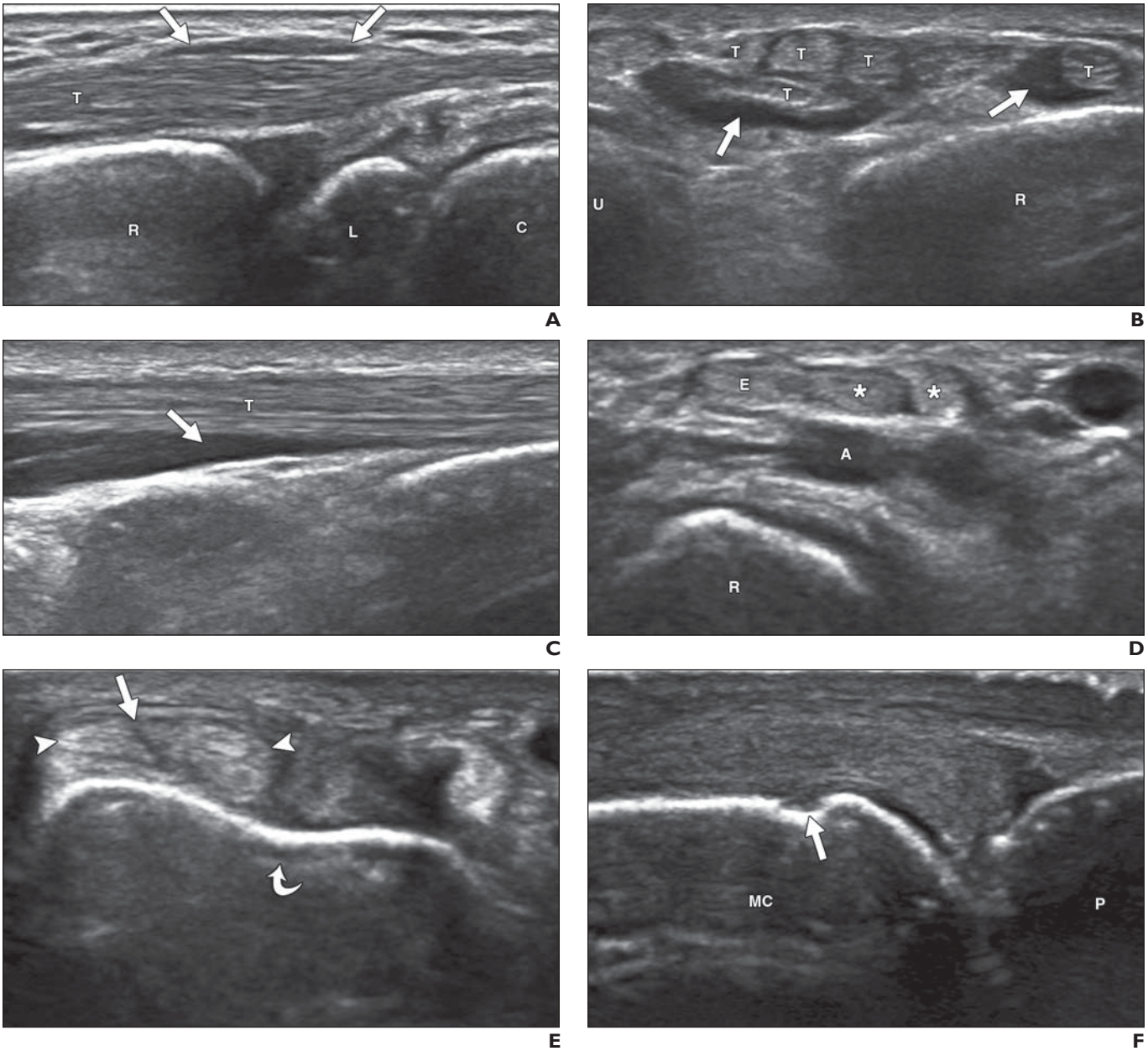

Fig. 1—48-year-old man in excellent health with asymptomatic wrist and hand.
A, Ultrasound image of dorsal wrist in sagittal plane shows normal extensor retinaculum (*arrows*). T = extensor digitorum tendon, R = radius, L = lunate, C = capitate.
B and **C,** Ultrasound images of dorsal wrist in axial (**B**) and sagittal (**C**) planes show normal tapering of hypoechoic muscle (*arrows*) at musculotendinous junction of extensor tendons (T). R = radius, U = ulna.
D, Ultrasound image of radial wrist in axial plane shows abductor pollicis longus tendon in short axis with multiple tendon slips (*asterisks*) or "lotus root" sign. E = extensor pollicis brevis tendon, R = radius, A = radial artery.
E, Ultrasound image of ulnar wrist in axial plane with hand supination shows extensor carpi ulnaris tendon (*arrowheads*) subluxation less than 50% from ulnar groove (*curved arrow*). Note hypoechoic cleft (*straight arrow*) as normal variant.
F, Ultrasound image of dorsal second metacarpophalangeal joint in sagittal plane shows pseudoerosion (*arrow*). MC = metacarpal, P = proximal phalanx.

(Fig. 1 continues on next page)

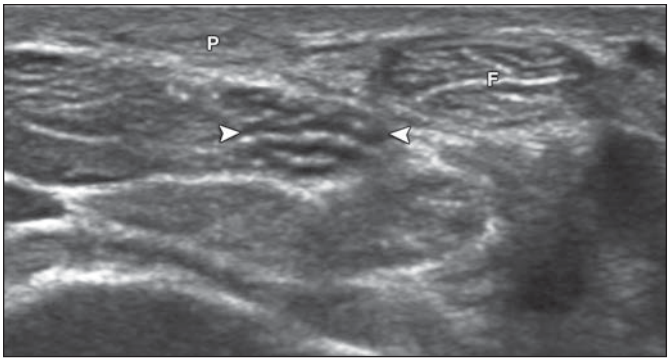

G

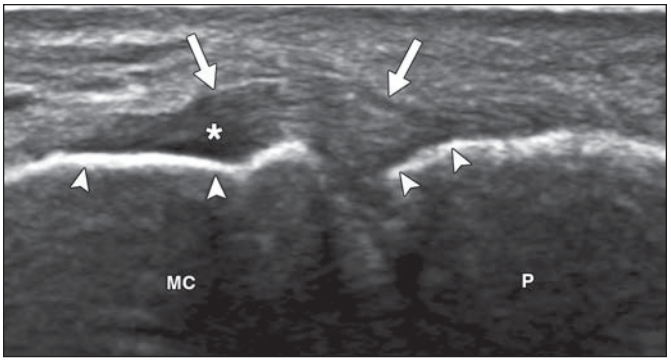

H

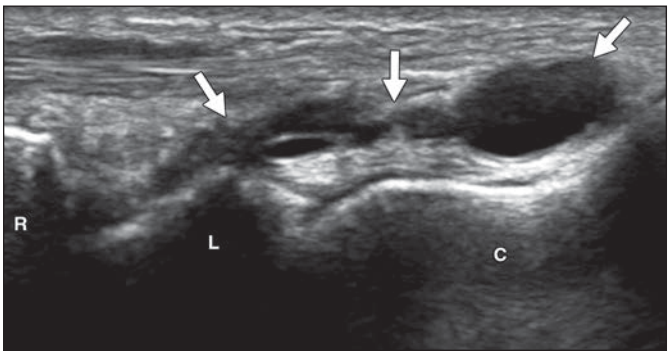

I

Fig. 1 (continued)—48-year-old man in excellent health with asymptomatic wrist and hand.
G, Ultrasound image of volar wrist in axial plane shows hypoechoic nerve fascicles and surrounding hyperechoic epineurium of median nerve (*arrowheads*). F = flexor carpi radialis, P = palmaris longus.
H, Ultrasound image of ulnar aspect of first metacarpophalangeal joint in coronal plane shows normal ulnar collateral ligament (*arrows*) and overlying adductor aponeurosis with characteristic bone contours (*arrowheads*) of metacarpal (MC) and proximal phalanx (P) at ligament attachment. Note anisotropy of proximal ligament fibers (*asterisk*).
I, Ultrasound image of dorsal wrist in sagittal plane shows multilocular anechoic ganglion cyst (*arrows*) with increased posterior through-transmission. R = radius, L = lunate, C = capitate.

musculotendinous junction as tenosynovitis (Fig. 1B), which can be avoided by confirming the normal tapering of muscle tissue in two imaging planes (Fig. 1C).

First extensor compartment—There are a number of normal variations that involve the wrist tendons that may simulate abnormalities, notably the first extensor compartment tendons [9]. Both the abductor pollicis longus and the extensor pollicis brevis may have multiple tendon slips that can simulate longitudinal clefts or tears. The abductor pollicis longus has multiple tendon slips in up to 95% of cases and is usually most apparent distal to the radius [10, 11]. The appearance of multiple tendon slips has been termed "the lotus root sign" because the multiple tendons appear similar to the appearance of a cut lotus root [10] (Fig. 1D). Multiple tendon fascicles may also but much less commonly involve the extensor pollicis brevis, described in less than 3–7% [10, 11]. Another possible variation of the first extensor wrist compartment is subcompartmentalization, with an incidence varying from 24% to 77.5% [11]. The presence of septation may cause complete subcompartmentalization of the extensor pollicis brevis and abductor pollicis longus tendon sheaths in 23% of cases. On ultrasound, an echogenic septation has been described in the setting of subcompartmentalization, although the septation may appear hypoechoic because of anisotropy; a small bony ridge between two osseous grooves at the attachment of the septation is often a more obvious finding [11]. Partial subcompartmentalization occurs in 9% of cases, which may make visualization of the septation with ultrasound difficult [10]. The presence of subcompartmentalization is important when injecting the first compartment tendon sheath for treatment of de Quervain tenosynovitis because incomplete filling of each compartment (when present) may result in ineffective treatment [11]. Another variation is absence of the extensor pollicis brevis tendon seen in 4.5% of cases [10].

Extensor carpi ulnaris—There are several potential diagnostic pitfalls related to the extensor carpi ulnaris tendon in the sixth extensor wrist compartment. A hypoechoic cleft may be seen when the extensor carpi ulnaris tendon is imaged in the short axis (Fig. 1E). A similar finding has been described at MRI, thought to represent fibrovascular tissue in between the two spiraling heads of the extensor carpi ulnaris [12–14]. The characteristic location, lack of tenosynovitis, and lack of symptoms help to differentiate this finding from a true longitudinal tendon tear. An accessory extensor digiti minimi tendon may also arise from the extensor carpi ulnaris, described in 34% of cases, which may produce an apparent tendon cleft [15]. Another potential pitfall relates to the position of the extensor carpi ulnaris within the ulnar

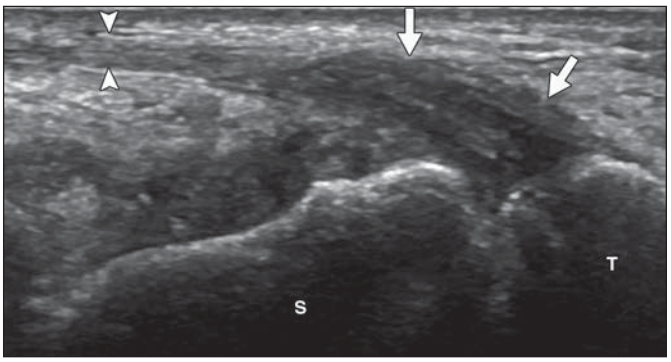

Fig. 2—67-year-old woman with flexor carpi radialis tendinosis. Ultrasound image in long axis to flexor carpi radialis tendon (*arrowheads*) shows hypoechoic tendinosis (*arrows*) and adjacent degenerative changes at scaphoid (S)–trapezium (T) articulation.

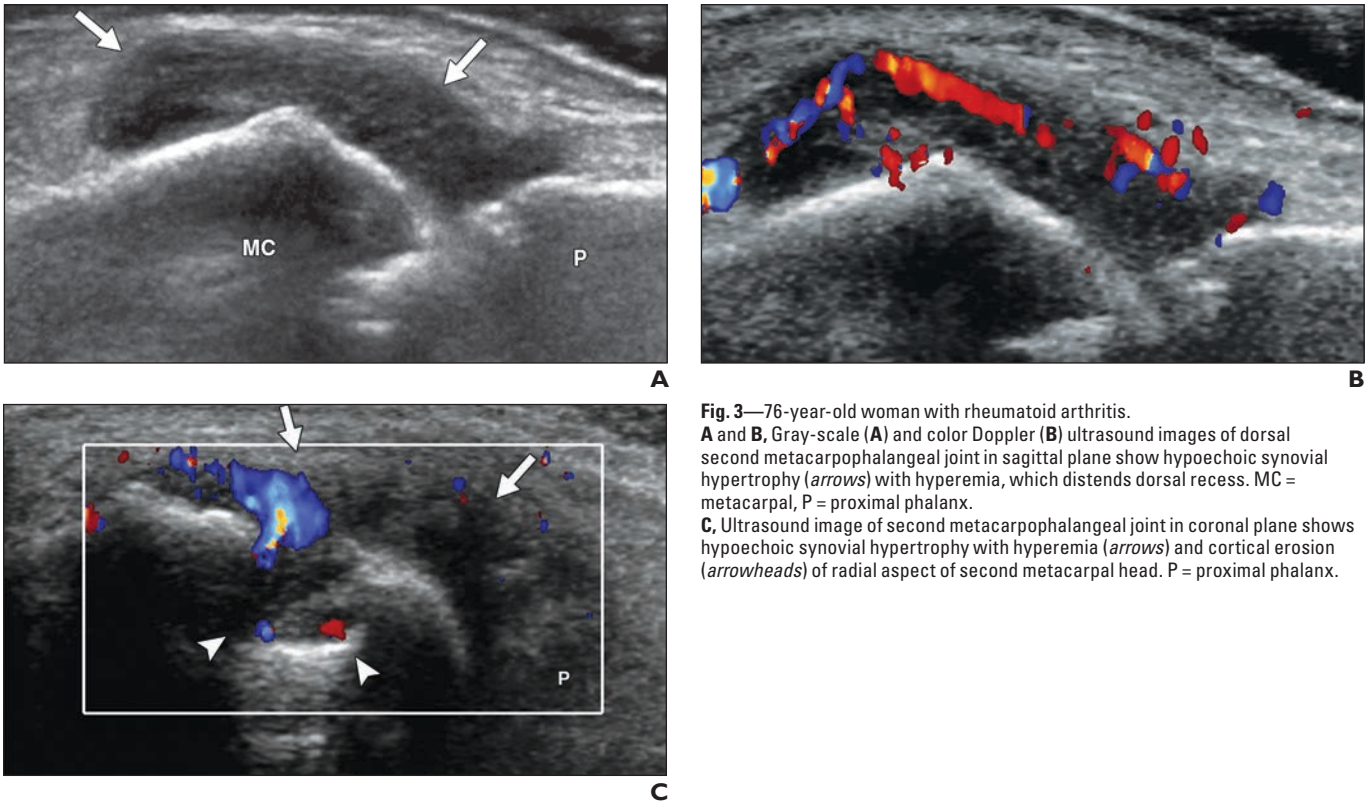

Fig. 3—76-year-old woman with rheumatoid arthritis.
A and **B**, Gray-scale (**A**) and color Doppler (**B**) ultrasound images of dorsal second metacarpophalangeal joint in sagittal plane show hypoechoic synovial hypertrophy (*arrows*) with hyperemia, which distends dorsal recess. MC = metacarpal, P = proximal phalanx.
C, Ultrasound image of second metacarpophalangeal joint in coronal plane shows hypoechoic synovial hypertrophy with hyperemia (*arrows*) and cortical erosion (*arrowheads*) of radial aspect of second metacarpal head. P = proximal phalanx.

groove. In pronation, the extensor carpi ulnaris tendon normally is located within this groove; however, with supination or wrist ulnar deviation there can normally be subluxation with the up to 50% of the extensor carpi ulnaris tendon located out of the groove [16] (Fig. 1E). The presence of tenosynovitis or subluxation greater than 50% of the tendon width should be considered abnormal.

Flexor carpi radialis—Another pitfall is incomplete evaluation of the flexor carpi radialis tendon. Although evaluation of the wrist tendons typically begins at the radiocarpal joint, it is important to assess the tendons distal to this level so as not to overlook an abnormality. One cause of wrist and hand pain is osteoarthritis at the scaphoid-trapezium-trapezoid (or triscaphe) joint. In the presence of osteoarthritis at these articulations, tendinosis and potential tear of the flexor carpi radialis may occur [17] (Fig. 2). Assessment of wrist or hand pain near the thumb should include examination of the flexor carpi radialis as well as the adjacent joint articulations at this site.

Inflammatory Arthritis

Ultrasound plays an important role in the assessment of inflammatory arthritis because it can help diagnose joint inflammation before initiation of arthritis treatment, assess response to treatment, and guide percutaneous aspiration or injection [18, 19].

Synovial Hypertrophy or Synovitis

The hallmark of inflammatory arthritis is synovial hypertrophy, which appears hypoechoic (Fig. 3A) or, less commonly, isoechoic or hyperechoic compared with subdermal fat [20]. Although the term "synovitis" is often used loosely, the term "synovial hypertrophy" may be more appropriate because the thickened synovium at imaging may not always be truly inflamed. This may explain the variable appearances of abnormal synovium at ultrasound. The term "synovitis" has been applied when the synovial hypertrophy is hypoechoic in the presence of synovial Doppler signal intensity [21]. Synovial hypertrophy can involve any synovial space, such as a joint recess or tendon sheath, and may show hyperemia on color or power Doppler imaging (Fig. 3B). The use of power Doppler imaging is advocated because it is more sensitive compared with conventional color Doppler imaging and is angle independent [22].

Evaluation for synovial hypertrophy requires a comprehensive assessment so as not to overlook pathologic findings. A search pattern should include the three articulations of the wrist (distal radioulnar, radiocarpal, and midcarpal) (Fig. 4), the metacarpophalangeal joints, and the interphalangeal joints. In the wrist joints, synovial hypertrophy is most often detected within the dorsal joint recesses [23]. With the metacarpophalangeal and interphalangeal joints, the dorsal recesses are targeted, although additional assessment of the volar recesses of the proximal interphalangeal joints has also been advocated [24]. Inflammatory synovial hypertrophy characteristically involves a recess of a synovial joint in a diffuse manner with resulting distention of the joint recesses. Although it is important to target the synovial spaces of the wrist and proximal hand when there is concern for rheumatoid arthritis (metacarpophalangeal and proximal interphalangeal joints), the distal interphalangeal joints should also be included to evaluate for other causes of inflammatory arthritis, such as psoriatic arthritis [25, 26]. The tendon sheaths should also be evaluated for synovial hypertrophy, especially the extensor carpi ulnaris [23, 27] (Fig. 4B).

Erosions

Bone erosions are another feature of inflammatory arthritis. They appear as a focal discontinuity of the bone surface visible in

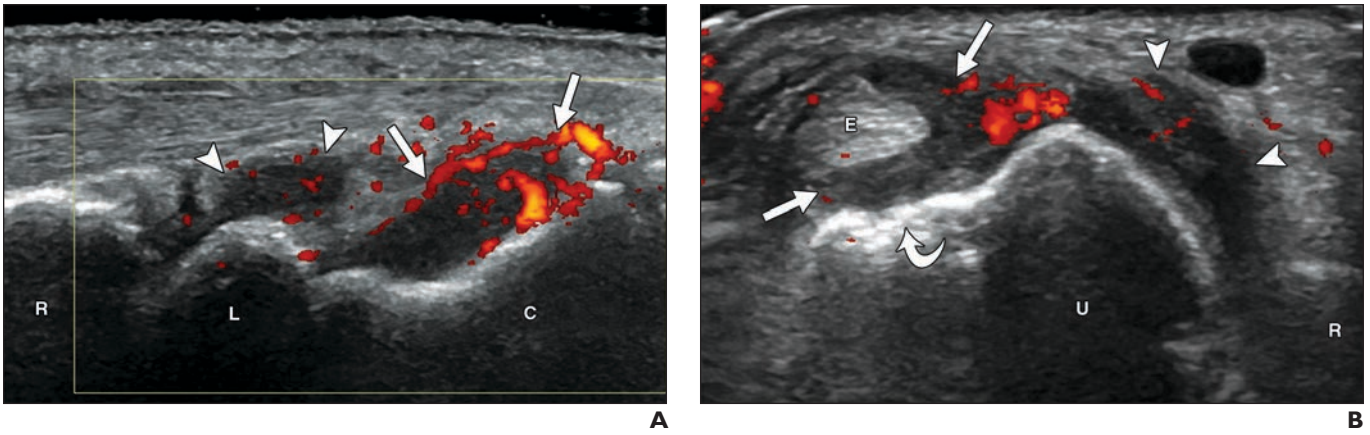

Fig. 4—75-year-old woman with rheumatoid arthritis.
A, Power Doppler ultrasound image of dorsal wrist in sagittal plane shows hypoechoic synovial hypertrophy with hyperemia of midcarpal (*arrows*) and radiocarpal (*arrowheads*) joint dorsal recesses. R = radius, L = lunate, C = capitate.
B, Power Doppler ultrasound image of ulnar wrist in axial plane shows extensor carpi ulnaris (E), hypoechoic tenosynovitis with hyperemia (*straight arrows*), and adjacent hypoechoic synovial hypertrophy of distal radioulnar joint (*arrowheads*). Note cortical erosions (*curved arrow*) of ulna (U). R = radius.

two perpendicular planes [20] (Fig. 3C). Once synovial hypertrophy is identified, a detailed search for erosions should be initiated to include all of the joint surfaces. At the metacarpal heads, the radial and ulnar aspects should be targeted. This is a significant limitation in the use of ultrasound because much of the bone surfaces cannot be visualized due to the approximation of other osseous structures. Thus, the sensitivity of ultrasound in the diagnosis of erosions is less than ideal (42%) but still higher than radiography (19%) although lower than MRI (68%) when compared with high-resolution CT [28]. The radial aspect of the second metacarpal and the ulnar aspect of the fifth metacarpal are two areas where erosions are commonly identified with ultrasound [23] (Fig. 3C).

Pitfalls

Detecting hyperemia—One pitfall is failure to detect hyperemia in the presence of synovial hypertrophy. Minimizing transducer pressure when assessing for hyperemia is important because excessive pressure may dampen blood flow; "floating" the transducer on a thick layer of gel or use of a standoff pad is helpful to avoid this pitfall. Other factors that can help detect hyperemia include lowering the velocity scale (or pulse repetition frequency) as far as possible without creating noise, lowering the filter (which is usually automatically adjusted with scale),

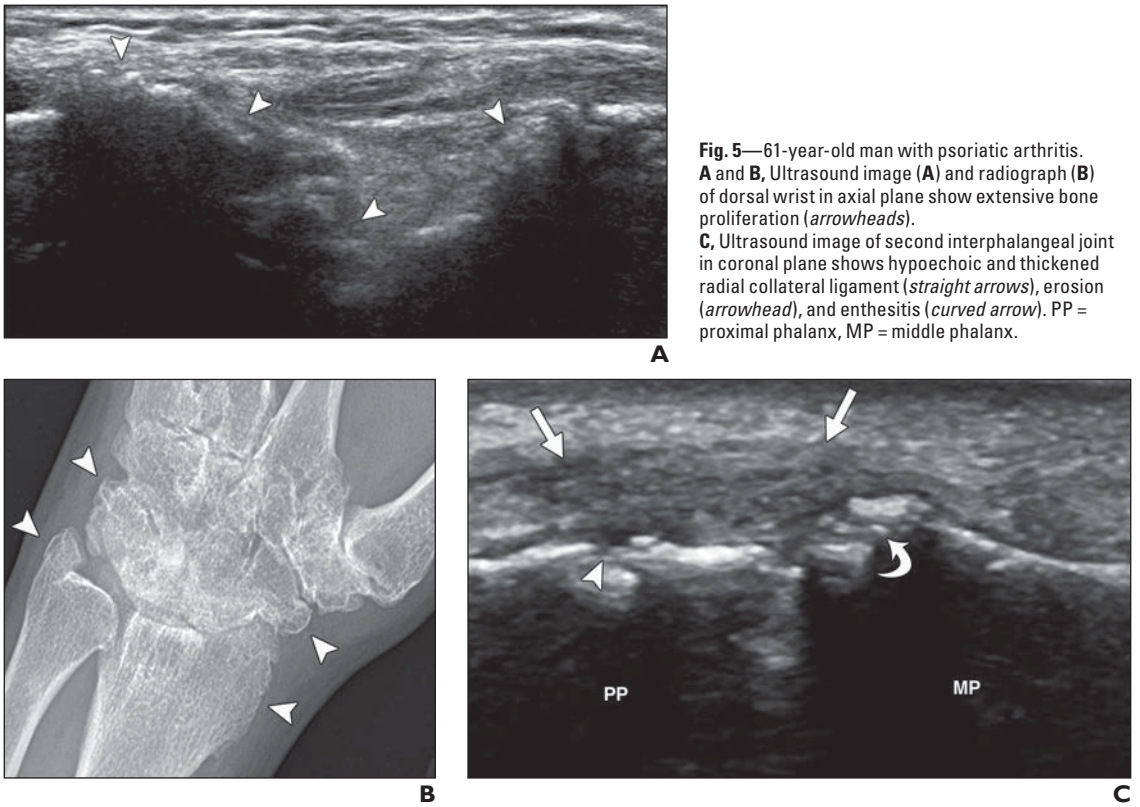

Fig. 5—61-year-old man with psoriatic arthritis.
A and **B,** Ultrasound image (**A**) and radiograph (**B**) of dorsal wrist in axial plane show extensive bone proliferation (*arrowheads*).
C, Ultrasound image of second interphalangeal joint in coronal plane shows hypoechoic and thickened radial collateral ligament (*straight arrows*), erosion (*arrowhead*), and enthesitis (*curved arrow*). PP = proximal phalanx, MP = middle phalanx.

and narrowing the ROI (which increases the frame rate). Color or power Doppler gain should be adjusted to a level just below the point where background artifact is visible. It is important to also be aware that synovial hypertrophy and hyperemia may be reduced if a patient is taking nonsteroidal antiinflammatory drugs [29].

Distinguishing erosions from other causes of cortical irregularity—In addition to relatively low sensitivity of ultrasound in the diagnosis of osseous erosions, ultrasound is also not very specific. When compared with high-resolution CT, ultrasound has a false-positive rate of 29% in the diagnosis of cortical erosions [30] because ultrasound is sensitive in identifying cortical irregularity but there are many causes for such findings.

One potential pitfall is termed the "pseudoerosion" of the metacarpal head. Although most commonly seen at the dorsal aspect of the second metacarpal, this finding is seen to variable degrees at every metacarpal (and metatarsal). The pseudoerosion is a smooth depression (mean depth, 0.3 mm) in the dorsal metacarpal cortex located at the margin of the hyaline articular cartilage at the site of the dorsal joint recess [31] (Fig. 1F). Although true erosion can involve this area, the finding of a shallow and smooth concavity in this characteristic location indicates a normal finding; absence of adjacent synovial hypertrophy is also a finding that supports that this finding is not a true erosion.

Bone irregularity may also be seen due to bone proliferation in psoriatic arthritis (Figs. 5A and 5B), osteophytes in osteoarthritis (Fig. 6), and after trauma. It is important to consider other imaging and clinical findings to add specificity to potential erosions seen at ultrasound. One finding is the presence of adjacent synovial hypertrophy, which adds specificity. It is also important to consider the distribution of the potential erosions, the findings at radiography, and clinical and laboratory findings.

Isolated synovial hypertrophy—Another pitfall is the finding of minimal synovial hypertrophy of a joint recess without hyperemia or erosions at ultrasound. This nonspecific finding when isolated may be seen in several situations and has been shown to be of little clinical relevance [32].

One scenario that may cause isolated synovial hypertrophy without hyperemia or erosions is early inflammatory arthritis. In the setting of isolated synovial hypertrophy (with negative rheumatoid factor and negative anticyclic citrullinated peptide and at least one swollen joint or increased C-reactive protein), one study has shown that the probability of inflammatory arthritis ranges from 0% to 39% [33]. With the additional finding of synovial hyperemia or erosions at ultrasound, this probability increases to 8–85% [33]. With the presence of all three ultrasound findings (synovial hypertrophy, hyperemia, and erosions), the probability of inflammatory arthritis increases further to 50–94% [33]. The distribution of ultrasound findings should also correlate with the expected sites of a specific inflammatory arthritis; for example, the synovial proliferation should involve the wrist or proximal hand with rheumatoid arthritis.

Other causes for nonspecific synovial hypertrophy without hyperemia or erosions include osteoarthritis, prior trauma, and other forms of inflammatory arthritis. Correlation with distribution and other ultrasound findings is again important; mild distal interphalangeal joint synovial hypertrophy with osteophytes can be explained by osteoarthritis as the cause. Correlation with clinical examination and laboratory findings is also essential to add specificity. Positive rheumatoid factor and anticyclic citrullinated peptide suggest that even nonspecific synovial hypertrophy without hyperemia or erosions makes the diagnosis of inflammatory arthritis probable [33]. In patients with rheumatoid arthritis, the finding of hyperemia predicts relapse and radiographic progression even with low levels of disease and subclinical inflammation [34].

Rheumatoid versus other types of inflammatory arthritis—One last pitfall in the use of ultrasound in evaluation for inflammatory arthritis of the hand and wrist is failure to consider other types of inflammatory arthritis and their key anatomic sites of involvement. Although involvement of synovial spaces (joint recesses and tendon sheaths) is common in inflammatory arthritis, other anatomic targets should include the entheses as well as other cortical surfaces beyond the joint articulations and their recesses. For example, psoriatic arthritis and the other seronegative spondyloarthropathies characteristically cause inflammatory enthesitis, which appears as irregular bone proliferation at the tendon and ligament attachments with possible erosions and adjacent hypoechoic inflammation and hyperemia [25, 26] (Fig. 5C). Because it is unrealistic to screen every enthesis of each hand given time constraints, often the clues

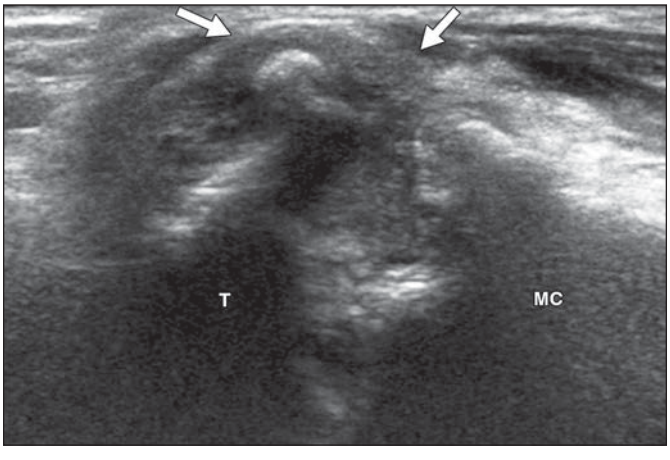

Fig. 6—60-year-old man with osteoarthritis. Ultrasound image of first carpometacarpal joint shows osteophytes and synovial hypertrophy (*arrows*). T = trapezium, MC = first metacarpal.

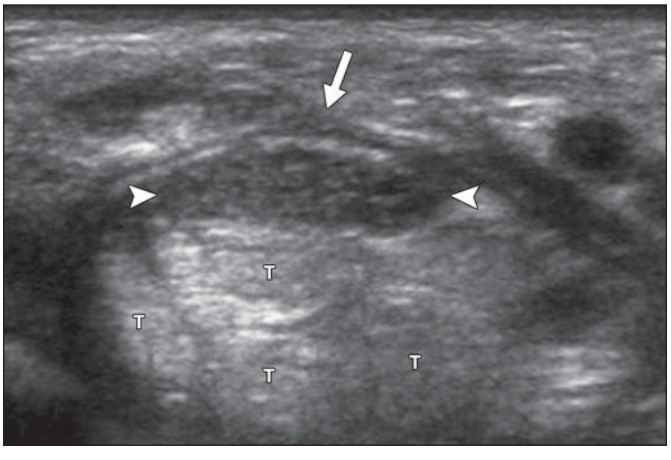

Fig. 7—51-year-old woman with prior surgical carpal tunnel release and continued symptoms. Ultrasound image of volar wrist in axial plane shows hypoechoic and enlarged median nerve (*arrowheads*) and hypoechoic thickened retinaculum (*arrow*). T = flexor tendons within carpal tunnel.

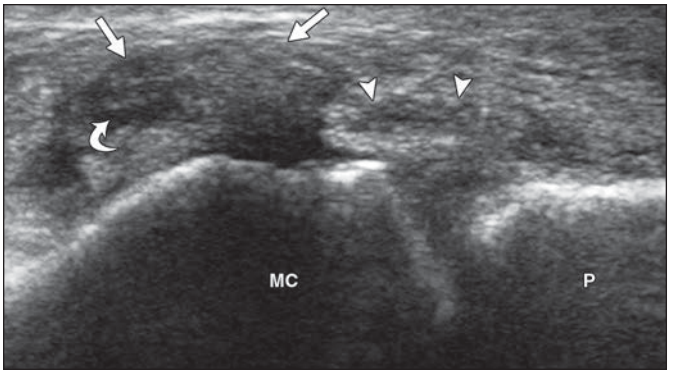

Fig. 8—58-year-old man with displaced ulnar collateral ligament tear (Stener lesion). Ultrasound image of ulnar aspect of first metacarpophalangeal joint in coronal plane shows displaced hypoechoic ligament (*straight arrows*) with stump directed proximally (*curved arrow*) and hypoechoic thickened adductor aponeurosis (*arrowheads*). MC = first metacarpal, P = proximal phalanx.

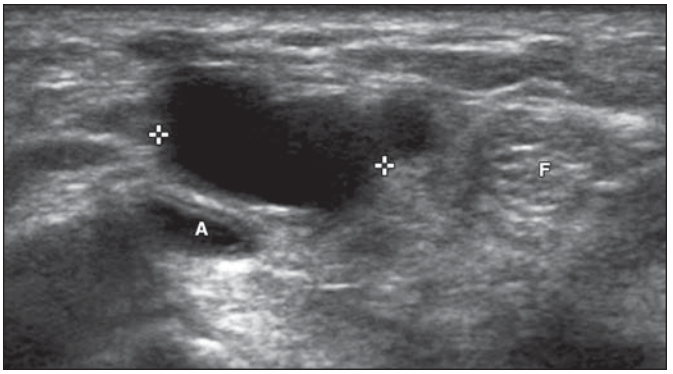

Fig. 9—61-year-old man with volar ganglion cyst. Ultrasound image of volar wrist in axial plane shows anechoic multilocular ganglion cyst (*cursors*) with increased posterior through-transmission. F = flexor carpi radialis, A = radial artery.

to a more focal ultrasound evaluation include abnormal radiographs (showing enthesitis or bone proliferation) and history and physical examination findings; a swollen or painful digit should include evaluation of the entheses. Cortical irregularity from periosteal new bone formation also can be seen in psoriatic arthritis at any osseous site (Figs. 5A and 5B). Another diagnostic consideration for bone irregularity is gout, which is characterized by the presence of periarticular bone erosion and adjacent hyperechoic tophus [35].

Carpal Tunnel Syndrome

Background

Ultrasound has been used to diagnose carpal tunnel syndrome for more than 20 years [36]. In addition, ultrasound has been shown to be the most cost-effective diagnostic test for carpal tunnel syndrome when a patient is referred from a specialist [37]. The characteristic ultrasound finding of any peripheral nerve entrapment is hypoechoic enlargement of the involved nerve at and just proximal to the entrapment site with distal tapering or transition to more normal size [36]. The median nerve, as other peripheral nerves, is ideally identified in the short axis where the hypoechoic nerve fascicles and surrounding hyperechoic connective tissue create a characteristic honeycomb appearance [38].

Pitfalls

Flexor carpi radialis and palmaris longus tendons—The adjacent flexor carpi radialis and palmaris longus tendons should not be mistaken as the median nerve given their proximity (Fig. 1G). In contrast to a normal peripheral nerve, a normal tendon will appear more hyperechoic with a fibrillar echotexture. A normal tendon will also show uniform anisotropy and appear diffusely hypoechoic when the transducer is toggled, unlike a peripheral nerve in which only the echogenic connective tissue elements surrounding the hypoechoic nerve fascicles show anisotropy. In addition, when followed proximally in the axial plane, the median nerve courses in a characteristic manner; the median nerve moves radial and then deep and ulnar in between the flexor digitorum superficialis and profundus, which is unlike the flexor carpi radialis and palmaris longus, which remain in the same superficial tissue planes [39].

Measurement technique and diagnostic criteria—In carpal tunnel syndrome, the median nerve is assessed for enlargement at the volar wrist crease at the level of the pisiform or flexor retinaculum. At this site, the median nerve area can be measured using the circumferential trace mode at the point of maximal enlargement, measured just inside the echogenic epineurium (Fig. 1G). The threshold area of the median nerve for diagnosing carpal tunnel syndrome is debated depending on how one selects the sensitivity and specificity. In general, less than 8 mm^2 is considered normal, 8–12 mm^2 is borderline, and greater than 12 mm^2 is abnormal [38]. One method to accurately diagnose carpal tunnel syndrome is to compare the area of the median nerve proximally (at the level of the proximal one third of the pronator quadratus) and distally where the nerve is most enlarged (at the wrist crease); enlargement of 2 mm^2 or greater results in 99% sensitivity and 100% specificity [40]. In the setting of a bifid median nerve (usually with a persistent median artery located in between the nerve bundles), the area should be added and 4 mm^2 used as the threshold compared with the median nerve size at the pronator quadratus [40].

Postoperative assessment—Additional pitfalls exist in the ultrasound assessment after carpal tunnel surgery. A common procedure used to treat carpal tunnel syndrome is surgical release of the carpal tunnel or flexor retinaculum. After such surgery, the retinaculum can have a variable appearance because the retinaculum may be hypoechoic and thickened and anterior displacement is common [41] (Fig. 7). It may be extremely difficult to differentiate a postoperative successful retinaculum release from an incomplete release or scar tissue. The significance of median nerve size after surgical treatment is controversial. Although the study by Abicalaf et al. [42] has shown that the median nerve area decreases after successful carpal tunnel release, Lee et al. [41] showed that the median nerve area increases in the distal carpal tunnel. Additionally, Naranjo et al. [43] showed that median nerve size as shown with ultrasound does not correlate with clinical outcome after surgery and therefore is of limited value.

Ulnar Collateral Ligament of Thumb

Background

Ultrasound can be used to effectively evaluate for ulnar collateral ligament injuries of the thumb (also termed "gamekeeper thumb" or "skier thumb") [44]. Importantly, ultrasound can diagnose a displaced ulnar collateral ligament tear (Stener lesion) with 100% accuracy when lack of normal ligament fibers is seen spanning the joint and there is a round heterogeneous masslike area identified proximal to the metacarpophalangeal joint [45].

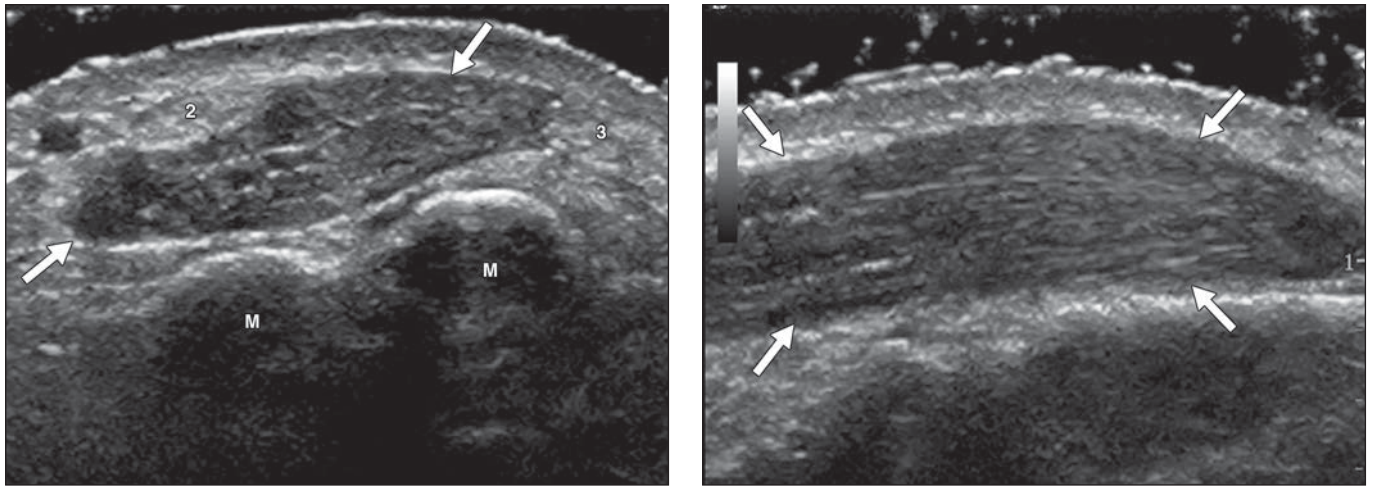

Fig. 10—32-year-old man with extensor digitorum brevis manus.
A and **B,** Ultrasound images of dorsal wrist in axial **(A)** and sagittal **(B)** planes show hypoechoic accessory muscle (*arrows*), which increased in size with active extension of fingers against resistance. 2 = second extensor tendon, 3 = third extensor tendon, M = metacarpal.

Pitfalls

Probe position—Selecting the correct probe position and anatomic plane is essential to ensure that the ligament fibers are in the imaging plane. The key to the proper anatomic plane is to identify the smooth concavities in the distal metacarpal and proximal phalanx because these are the footprints of the ligament fiber attachments (Fig. 1H) [45].

Adductor aponeurosis—A second pitfall is mistaking the injured adductor aponeurosis as intact ulnar collateral ligament fibers. In the setting of a Stener lesion, the proximal edge of the adductor aponeurosis is often injured and appears hypoechoic and thickened on ultrasound (Fig. 8). Soft-tissue swelling and hematoma may also create a somewhat heterogeneous appearance to the area; however, the presence of the adductor aponeurosis can easily be confirmed with passive flexion of the interphalangeal joint [45]. With this dynamic maneuver, the adductor aponeurosis can be identified gliding back and forth over the metacarpophalangeal joint with movement of the extensor tendon.

Stener lesion—A third pitfall relates to the misconception that the displaced ulnar collateral ligament must be located superficial to the adductor aponeurosis. The key feature of a displaced ulnar collateral ligament tear (Stener lesion) is a rolled-up appearance at the leading edge of the proximal adductor aponeurosis (Fig. 8). The proximal stump may be located at the leading edge of the aponeurosis, superficial to the aponeurosis, or more proximal along the metacarpal [45].

Ganglion Cyst

Ganglion cysts account for 50–70% of soft-tissue masses around the wrist [46]. The pitfalls in the ultrasound diagnosis of ganglion cysts include uncertainty in ultrasound criteria and incomplete evaluation. Ganglion cysts at the wrist are commonly anechoic or hypoechoic and multilocular with increased posterior through-transmission, although they often appear complex [47]. Ganglion cysts that are 10 mm in size or smaller are more likely to be hypoechoic, although a multilocular or multilobular appearance is still present without an associated soft-tissue mass [46]. The two most common locations where ganglion cysts occur include superficial to the dorsal component of the scapholunate ligament (Fig. 1I) and volar between the radial artery and flexor carpi radialis (Fig. 9). Ultrasound evaluation of the wrist should include these two anatomic locations. The dorsal ganglion cyst should be differentiated from a distended radiocarpal joint dorsal recess because the two may appear similar. A dorsal ganglion cyst is usually multilocular with little compressibility, which is different from a distended radiocarpal joint dorsal recess that is unilocular and compressible with transducer pressure or joint movement. When a volar ganglion cyst is located immediately adjacent to the radial artery, transmitted pulsatile movement of the ganglion cyst should not be misinterpreted as a pseudoaneurysm.

Pseudomasses

There are several variations in the muscles that traverse the wrist that may present clinically as a soft-tissue mass [48]. One example is the extensor digitorum brevis manus. This accessory muscle is located dorsally at the wrist at the ulnar aspect of the second extensor tendon in between the second and third extensor tendons, has a prevalence of 2–3%, and is bilateral in 54% of cases [49]. At ultrasound, the characteristic appearance of hypoechoic muscle fibers and interspersed hyperechoic fibrofatty septations is essential, along with the specific location of this accessory muscle (Fig. 10). In addition, enlargement of the muscle belly with active finger extension against resistance is characteristic [49]. Another muscle variant that may present as a pseudotumor is an inverted palmaris longus, termed the "palmaris longus inversus" variant [48]. In this scenario, the muscle belly of the palmaris longus is located distal and the tendon proximal. Similarly, the characteristic echotexture of muscle should be seen as well as an anatomic location continuous with the palmaris longus tendon that will enable an accurate diagnosis. Other variations of the palmaris longus include bifid, digastric, and nontendinous variants as well as absence [48].

Conclusion

Although ultrasound has been shown to be an effective imaging method for assessment of many pathologic conditions of the wrist, knowledge of the potential pitfalls is essential to avoid misdiagnosis and achieve high diagnostic accuracy.

References

1. Olubaniyi BO, Bhatnagar G, Vardhanabhuti V, Brown SE, Gafoor A, Suresh PS. Comprehensive musculoskeletal sonographic evaluation of the hand and wrist. *J Ultrasound Med* 2013; 32:901–914
2. Tagliafico A, Rubino M, Autuori A, Bianchi S, Martinoli C. Wrist and hand ultrasound. *Semin Musculoskelet Radiol* 2007; 11:95–104
3. Klauser AS, Tagliafico A, Allen GM, et al. Clinical indications for musculoskeletal ultrasound: a Delphi-based consensus paper of the European Society of Musculoskeletal Radiology. *Eur Radiol* 2012; 22:1140–1148
4. Daenen B, Houben G, Bauduin E, Debry R, Magotteaux P. Sonography in wrist tendon pathology. *J Clin Ultrasound* 2004; 32:462–469
5. Martinoli C, Derchi LE, Pastorino C, Bertolotto M, Silvestri E. Analysis of echotexture of tendons with US. *Radiology* 1993; 186:839–843
6. Resnick D. Roentgenographic anatomy of the tendon sheaths of the hand and wrist: tenography. *Am J Roentgenol Radium Ther Nucl Med* 1975; 124:44–51
7. Robertson BL, Jamadar DA, Jacobson JA, et al. Extensor retinaculum of the wrist: sonographic characterization and pseudotenosynovitis appearance. *AJR* 2007; 188:198–202
8. Massaki AN, Tan J, Huang BK, Chang EY, Trudell DJ, Resnick DL. Extensor retinaculum of the wrist: gross anatomical correlation with MR imaging after ultrasound-guided tenography with emphasis on anatomical features in wrist dorsiflexion responsible for tendon impingement. *Skeletal Radiol* 2013; 42:1727–1737
9. De Maeseneer M, Marcelis S, Jager T, Girard C, Gest T, Jamadar D. Spectrum of normal and pathologic findings in the region of the first extensor compartment of the wrist: sonographic findings and correlations with dissections. *J Ultrasound Med* 2009; 28:779–786
10. Choi SJ, Ahn JH, Lee YJ, et al. de Quervain disease: US identification of anatomic variations in the first extensor compartment with an emphasis on subcompartmentalization. *Radiology* 2011; 260:480–486
11. Rousset P, Vuillemin-Bodaghi V, Laredo JD, Parlier-Cuau C. Anatomic variations in the first extensor compartment of the wrist: accuracy of US. *Radiology* 2010; 257:427–433
12. Kalson NS, Malone PS, Bradley RS, Withers PJ, Lees VC. Fibre bundles in the human extensor carpi ulnaris tendon are arranged in a spiral. *J Hand Surg Eur Vol* 2012; 37:550–554
13. Pfirrmann CW, Zanetti M. Variants, pitfalls and asymptomatic findings in wrist and hand imaging. *Eur J Radiol* 2005; 56:286–295
14. Timins ME, O'Connell SE, Erickson SJ, Oneson SR. MR imaging of the wrist: normal findings that may simulate disease. *RadioGraphics* 1996; 16:987–995
15. Nakashima T. An accessory extensor digiti minimi arising from extensor carpi ulnaris. *J Anat* 1993; 182:109–112
16. Lee KS, Ablove RH, Singh S, De Smet AA, Haaland B, Fine JP. Ultrasound imaging of normal displacement of the extensor carpi ulnaris tendon within the ulnar groove in 12 forearm-wrist positions. *AJR* 2009; 193:651–655
17. Parellada AJ, Morrison WB, Reiter SB, et al. Flexor carpi radialis tendinopathy: spectrum of imaging findings and association with triscaphe arthritis. *Skeletal Radiol* 2006; 35:572–578
18. Backhaus M, Burmester GR, Gerber T, et al. Guidelines for musculoskeletal ultrasound in rheumatology. *Ann Rheum Dis* 2001; 60:641–649
19. Lopez-Ben RR. Assessing rheumatoid arthritis with ultrasound of the hands. (video article) *AJR* 2011; 197:W422
20. Wakefield RJ, Balint PV, Szkudlarek M, et al. Musculoskeletal ultrasound including definitions for ultrasonographic pathology. *J Rheumatol* 2005; 32:2485–2487
21. Iagnocco A, Naredo E, Wakefield R, et al. Responsiveness in rheumatoid arthritis: a report from the OMERACT 11 ultrasound workshop. *J Rheumatol* 2014; 41:379–382
22. Rubin JM, Bude RO, Carson PL, Bree RL, Adler RS. Power Doppler US: a potentially useful alternative to mean frequency-based color Doppler US. *Radiology* 1994; 190:853–856
23. Ohrndorf S, Halbauer B, Martus P, et al. Detailed joint region analysis of the 7-joint ultrasound score: evaluation of an arthritis patient cohort over one year. *Int J Rheumatol* 2013; 2013:493848
24. Vlad V, Berghea F, Libianu S, et al. Ultrasound in rheumatoid arthritis - volar versus dorsal synovitis evaluation and scoring. *BMC Musculoskelet Disord* 2011; 12:124
25. Gutierrez M, Filippucci E, De Angelis R, Filosa G, Kane D, Grassi W. A sonographic spectrum of psoriatic arthritis: "the five targets." *Clin Rheumatol* 2010; 29:133–142
26. Kaeley GS. Review of the use of ultrasound for the diagnosis and monitoring of enthesitis in psoriatic arthritis. *Curr Rheumatol Rep* 2011; 13:338–345
27. Navalho M, Resende C, Rodrigues AM, et al. Bilateral MR imaging of the hand and wrist in early and very early inflammatory arthritis: tenosynovitis is associated with progression to rheumatoid arthritis. *Radiology* 2012; 264:823–833
28. Døhn UM, Ejbjerg BJ, Court-Payen M, et al. Are bone erosions detected by magnetic resonance imaging and ultrasonography true erosions? A comparison with computed tomography in rheumatoid arthritis metacarpophalangeal joints. *Arthritis Res Ther* 2006; 8:R110
29. Zayat AS, Conaghan PG, Sharif M, et al. Do non-steroidal anti-inflammatory drugs have a significant effect on detection and grading of ultrasound-detected synovitis in patients with rheumatoid arthritis? Results from a randomised study. *Ann Rheum Dis* 2011; 70:1746–1751
30. Finzel S, Ohrndorf S, Englbrecht M, et al. A detailed comparative study of high-resolution ultrasound and micro-computed tomography for detection of arthritic bone erosions. *Arthritis Rheum* 2011; 63:1231–1236
31. Boutry N, Larde A, Demondion X, Cortet B, Cotten H, Cotten A. Metacarpophalangeal joints at US in asymptomatic volunteers and cadaveric specimens. *Radiology* 2004; 232:716–724
32. Witt M, Mueller F, Nigg A, et al. Relevance of grade 1 gray-scale ultrasound findings in wrists and small joints to the assessment of subclinical synovitis in rheumatoid arthritis. *Arthritis Rheum* 2013; 65:1694–1701
33. Freeston JE, Wakefield RJ, Conaghan PG, Hensor EM, Stewart SP, Emery P. A diagnostic algorithm for persistence of very early inflammatory arthritis: the utility of power Doppler ultrasound when added to conventional assessment tools. *Ann Rheum Dis* 2010; 69:417–419
34. Foltz V, Gandjbakhch F, Etchepare F, et al. Power Doppler ultrasound, but not low-field magnetic resonance imaging, predicts relapse and radiographic disease progression in rheumatoid arthritis patients with low levels of disease activity. *Arthritis Rheum* 2012; 64:67–76
35. Girish G, Glazebrook KN, Jacobson JA. Advanced imaging in gout. *AJR* 2013; 201:515–525
36. Klauser AS, Faschingbauer R, Bauer T, et al. Entrapment neuropathies II: carpal tunnel syndrome. *Semin Musculoskelet Radiol* 2010; 14:487–500
37. Fowler JR, Maltenfort MG, Ilyas AM. Ultrasound as a first-line test in the diagnosis of carpal tunnel syndrome: a cost-effectiveness analysis. *Clin Orthop Relat Res* 2013; 471:932–937
38. Peetrons PA, Derbali W. Carpal tunnel syndrome. *Semin Musculoskelet Radiol* 2013; 17:28–33
39. Jamadar DA, Jacobson JA, Hayes CW. Sonographic evaluation of the median nerve at the wrist. *J Ultrasound Med* 2001; 20:1011–1014
40. Klauser AS, Halpern EJ, De Zordo T, et al. Carpal tunnel syndrome assessment with US: value of additional cross-sectional area measurements of the median nerve in patients versus healthy volunteers. *Radiology* 2009; 250:171–177
41. Lee CH, Kim TK, Yoon ES, Dhong ES. Postoperative morphologic analysis of carpal tunnel syndrome using high-resolution ultrasonography. *Ann Plast Surg* 2005; 54:143–146
42. Abicalaf CA, de Barros N, Sernik RA, et al. Ul-

trasound evaluation of patients with carpal tunnel syndrome before and after endoscopic release of the transverse carpal ligament. *Clin Radiol* 2007; 62:891–894, discussion 895–896

43. Naranjo A, Ojeda S, Rua-Figueroa I, Garcia-Duque O, Fernandez-Palacios J, Carmona L. Limited value of ultrasound assessment in patients with poor outcome after carpal tunnel release surgery. *Scand J Rheumatol* 2010; 39:409–412
44. Ebrahim FS, De Maeseneer M, Jager T, Marcelis S, Jamadar DA, Jacobson JA. US diagnosis of UCL tears of the thumb and Stener lesions: technique, pattern-based approach, and differential diagnosis. *RadioGraphics* 2006; 26:1007–1020
45. Melville D, Jacobson JA, Haase S, Brandon C, Brigido MK, Fessell D. Ultrasound of displaced ulnar collateral ligament tears of the thumb: the Stener lesion revisited. *Skeletal Radiol* 2013; 42:667–673
46. Wang G, Jacobson JA, Feng FY, Girish G, Caoili EM, Brandon C. Sonography of wrist ganglion cysts: variable and noncystic appearances. *J Ultrasound Med* 2007; 26:1323–1328; quiz, 1330–1331
47. Teefey SA, Dahiya N, Middleton WD, Gelberman RH, Boyer MI. Ganglia of the hand and wrist: a sonographic analysis. *AJR* 2008; 191:716–720
48. Timins ME. Muscular anatomic variants of the wrist and hand: findings on MR imaging. *AJR* 1999; 172:1397–1401
49. Ouellette H, Thomas BJ, Torriani M. Using dynamic sonography to diagnose extensor digitorum brevis manus. *AJR* 2003; 181:1224–1226

FOR YOUR INFORMATION

Mark your calendar for the following ARRS annual meetings:
April 19–24, 2015—Toronto Convention Centre, Toronto, ON, Canada
April 17–22, 2016—Los Angeles Convention Center, Los Angeles, CA
April 30–May 5, 2017—Hyatt Regency New Orleans, New Orleans, LA
April 22–27, 2018—Marriott Wardman Park Hotel, Washington DC